WORLD CONFERENCE ON TIMBER ENGINEERING 2025
BRISBANE, AUSTRALIA
Advancing Timber for the Future Built Environment

Dynamic and long-term performance of friction-based connectors with wooden dowels.

Yoshiaki Wakashima [1], Hidemaru Shimizu [2], Akihisa Kitamori [3], Doppo Matsubara [4], Shingo Hanai[5] Mitsuo Fukumoto [6]

ABSTRACT: Shear walls in wood construction typically exhibit pinched hysteresis loop resulting in limited energy absorption, which is important for seismic performance. Thus, in order to develop a connection with high energy absorption using wood friction, shake table tests of a shear wall with friction-base connectors were conducted. To evaluate a long-term performance of the wood clamping force that generates the frictional force in an analytical model, coefficients related to pure creep and mechano-sorptive creep, which are required in the model, were obtained. Using these coefficients, the loss of wood clamping force under temperature and humidity fluctuations was evaluated by the analytical model. This paper presents the results of these tests and analyses.

KEYWORDS: wood friction, shake table test, time-dependent test, losses

1 – INTRODUCTION

This paper presents the dynamic performance of friction-based connectors by shake table tests, as well as various long-term tests and analytical evaluations.

2 – BACKGROUND

In Japan, an earthquake-prone country, shear walls using nailed sheathing panels are commonly used as earthquake resistant system in wooden buildings. However, nail joints exhibit pinched hysteresis loops for cyclic loading, which limits their energy absorption. The authors have been developing friction-based connectors using wood with excellent energy absorption to improve the seismic performance of wooden buildings [1, 2]. Since the friction based-connectors generates frictional force by clamping a steel plate between wood, we developed a specification that uses a wooden dowel to clamp in the direction parallel to the grain to ensure long-term performance [3]. We reported that a wall with the friction-based connectors using wood dowels significantly reduces seismic response compared to the nailed wood shear wall by shake table tests [3]. Long-term performance was also reported to be expected from time-dependent tests over multiple years [3]. However, in order to make friction-based connectors practical, it is necessary to evaluate the dynamic performance of the connector in more detail and to be able to quantify the long-term performance over the life of a structure. Accordingly, shake table tests of a wall with the connectors and tests to obtain various coefficients necessary to predict the long-term performance were performed.

3 – EXPERIMENTAL SETUP

3.1 SHAKE TABLE TESTS

The friction-based connectors are made by inserting dry-shrunk wooden dowels (white oak) into the studs and tightening a steel plate between them, as shown in Fig. 1. Wooden dowels were dried at 70°C and inserted into the studs without adhesive. Bolts were tightened by pulling the bolt tip with a centre hole cylinder and checking the pulling force with a pressure gauge and a pipe-type load

[1] Yoshiaki Wakashima, Toyama Prefectural Agricultural, Forestry and Fisheries Research Center, Imizu, Japan, yoshiaki.wakashima@pref.toyama.lg.jp

[2] Hidemaru Shimizu, School of Life Studies Sugiyama Jogakuen Univ., Nagoya, Japan, hidemaru@sugiyama-u.ac.jp

[3] Akihisa Kitamori, dept. Osaka Sangyo Univ., Daito, Japan, kitamori@ce.osaka-sandai.ac.jp

[4] Doppo Matsubara, Tokyo Univ. Agriculture and Technology, Fuchu, Japan, ft2661@go.tuat.ac.jp

[5] Shingo Hanai, evoltz Co., Ltd., Hamamatsu, Japan, s-hanai@chihiro.co.jp

[6] Mitsuo Fukumoto, evoltz Co, Ltd., Hamamatsu, Japan, fukumotomituo@gmail.com

https://doi.org/10.52202/080513-0014

cell. The studs and steel plates were joined to the columns and sheathing material of the shear wall as shown in Fig. 2. Detail of the connector and studs with the wooden dowels are shown in Fig. 3 and 4.

Shak table tests were conducted on a one-story shear wall specimen that was a combination of the friction wall and plywood walls. The test method is the same as previously reported [2]. As in previous reports, the shake table test was carried out by placing and fixing the wall specimen in the centre of a wood frame supporting a weight and allowing the specimen to bear the horizontal forces caused by the shaking (Fig. 5). The input ground motions were four times alternating 41% and 91% of the artificial building standard law of Japan wave (BSL), followed by two times of 100% BSL.

3.2 TIME-DEPENDENT TESTS

The post-tension loss analysis model developed by Fragiacomo and Davies [4] is applied to evaluate the decrease in wood clamping force over time. The

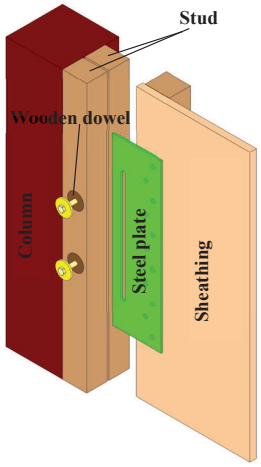

Figure.1 Friction-based connector with wooden dowel.

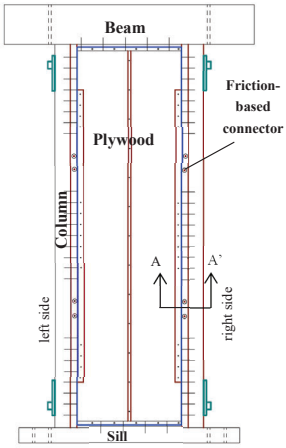

Figure 2. Schematic of shear wall with the connectors.

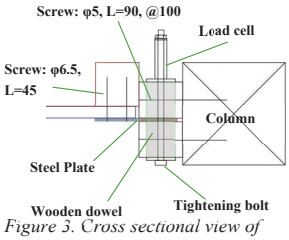

Figure 3. Cross sectional view of connector (A-A'). See Fig. 2.

Figure 4. Studs with wooden dowels.

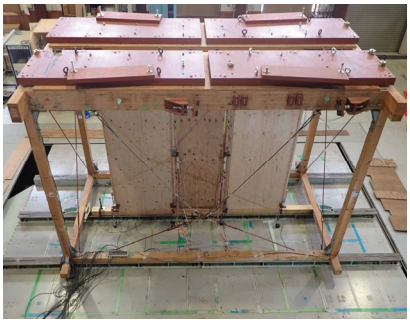

Figure 5. Shake table test setup.

Tabel 1: Summary of white oak specimen in cotrolled environment

Specimens	Dimension (mm)	Stress (MPa)	Density (kg/m^3)	Bolt	Washer	No. of specimens
WO-○12	φ30, L40	10	752	M6	t12	3
WO-○3	φ30, L40	9.5	751	M6	t3	3
WO-□12	26×26, L40	9.5	812	M6	t12	3
WO-○-Cp	φ30, L40	8.7	704			3

Tabel 2: Summary of Sugi specimen in controlled environment

Specimens	Dimension (mm)	Stress (MPa)	Density (kg/m^3)	Bolt	Washer	No. of specimens
SG-L	40×40×L80	8.5	405	M12	t12	3
SG-M	40×45×L30	13	308	M6	t3+t3.2	3
SG-L-Cp	45×45×L90	8	365			1
SG-M-Cp	30×30×L90	14.5	374			1

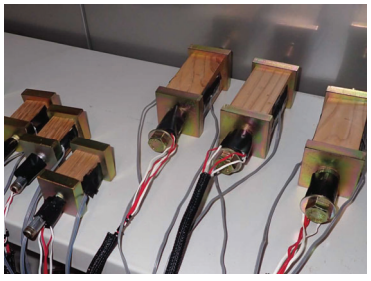

Figure 6. Prestress specimens.

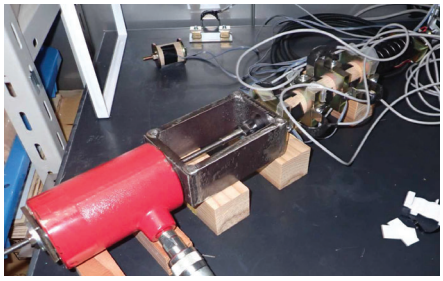

(a) White oak specimens

(b) Sugi specimens

Figure 7. Creep tests in controlled environment.

https://doi.org/10.52202/080513-0014

analytical model requires coefficients for pure creep and mechano-sorptive creep of a wood. In this report, pure creep was obtained from prestressing wood specimens under constant temperature and humidity conditions by back-calculating with the analytical model. Creep related to mechano-sorptive was determined from the prestressing wood under cyclic humidity conditions (20℃, 85% ⇔ 45%).

3.2.1 CREEP TEST

The prestressed specimens were white oak (WO) and Sugi (Cryptomeria japonica D. Don, SG). Two types of white oak specimens, one with a cross section of φ30 and an axial direction length of 40 mm (L40) and the other with a cross section of 26 x 26 mm, L40, were sandwiched between 12 mm (t12) thick steel plates or 3 mm (t3) washers and tightened with M6 bolts through the pipe-type load cell (Fig. 6). Two types of Sugi specimens, one with a cross section of 40 x 40 mm and an axial length of 80 mm (L80) and the other with a cross section of 40 x 45 mm and an axial length of 30 mm (L30), were sandwiched between t12 steel plates or 3+3.2 mm (t3+t3.2) washers and tightened with M12 or M6 bolts through the pipe-type load cell (Fig. 6). Creep tests (cp) were also conducted by stacking wood specimens and applying a constant load (8.5 MPa) with strong springs, as shown in Fig. 7. The specimens are white oak with φ30 , L40 and Sugi with cross-sections of 45 x 45 mm and 30 x 30 mm with L90. Summary of the specimens are shown in Tables 1 and 2. Tightening was basically performed as shown in Fig. 7(a), using an oil jack to pull the bolt with the prescribed load, lightly tightening the nut and then removing the jack.

3.2.2 CREEP TEST IN CYCLIC HUMIDITY

Cycle humidity tests were performed by clamping Sugi (Cy-SG25) and white oak (Cy-WO40) through the load cells with bolts, as shown in Fig. 8. In Cy-SG25, assuming a member with three connections in a row, three φ30 Sugi wood dowels were inserted in the centre of a 40×45×550 Sugi stud, glued with urethane adhesive and tightened at these wooden dowels. Summary of the test is given in Table 3. The test conditions consisted of applying the prescribed tightening force for 19 days at 20°C/65%, followed by five cycles of 85% and 45% relative humidity at one-week intervals, after which the transition of the tightening force was measured until the moisture content stabilised at 20°C/65%. Moisture contents were monitored on dummy test specimens placed in the same environment as the test specimens.

3.2.3 PRESTRESS TEST IN UNCONTROLED ENVIRONMENT

Prestress tests were conducted on Sugi and white oak in an indoor environment to evaluate prestress losses under uncontrolled temperature and humidity conditions. Summary of the tests are shown in Table 4. The specimens are shown in Fig. 9 and, as in the cyclic humidity test, the wood was bolted through the load cell. In V-2WO38, a steel plate was placed between studs in which white oak wooden dowels were inserted and the dowels were tightened with bolts, as shown in Fig. 9(b), to simulate a real friction joint.

4 – RESULTS

4.1 SHAKE TABLE TESTS

The lateral load-displacement relationship obtained from the one-story shake table test showed the pinched hysteresis response but larger area loops, as shown in the Fig. 10. The responses of the wood friction and plywood shear walls calculated from the strain gauges attached to the plywood are shown in the Fig. 11. The friction wall

Tabel3: Summary of creep tests in cyclic humidity

Designation of specimens	Dimension (mm)	Density (kg/m^3)	Initial stress (MPa)	Bolt	Washer	Number of specimens
Cy-SG	φ30, L25	321	7.48	M6	φ30t3	3
Cy-WO	φ30, L40	711	12.5	M6	φ30t3	3

Tabe 4: Summary of prestress tests in uncontrolled environment

Designation of specimens	Cross section (mm)	Density (kg/m^3)	Initial stress (MPa)	Bolt	Steel plates	Number of specimens
V-SG-L	40×45×L30	314	7.5	M6	φ30t3	2
V-SG-M	40×45×L30	315	13.6	M6	φ30t3	3
V-2WO	φ30, L30×2	781	10.8	M6	φ30t3	2
V-JO-R	φ30, L36	637	10.8	M6	φ30t3	2
V-JO-R-A	φ30, L36	646	10.8	M6	φ30t3	2

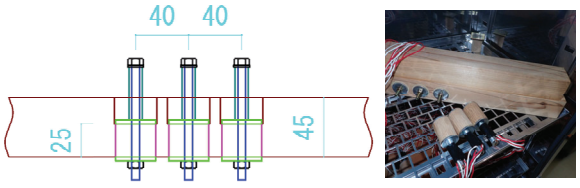

(a) Cy-SG25 (b) Cy-WO40

Figure 8 Creep tests in cyclic humidity.

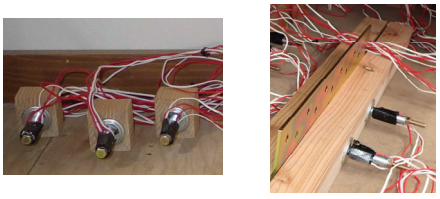

(a)V-SG30 (b)V-2WO38

Figure 9 Prestress tests in uncontrolled environment.

https://doi.org/10.52202/080513-0014

and plywood walls exhibited bilinear and typical pinched hysteresis loop responses, respectively. The relationship between the displacement of the friction-based connectors and the lateral load on the woood friction wall is shown in Fig. 12, which is also bilinear hysteresis loops without pinching behavior. Since the load-bearing elements of the friction wall are almost exclusively friction-based connectors, the hysteresis loop of the friction wall reflects the characteristics of the connectors.

Clamping force of the connections at the end of each input and lateral load at 1 mm of the connection displacement are shown in the Fig. 13. The maximum response displacements for each input are also shown in the figure. Fig. 13 shows that the clamping force did not decrease unless the past maximum response displacement was exceeded, and tended to decrease when it was exceeded. The clamping force showed an overall decreasing trend as the input progressed, but there was almost no decrease in the lateral load, the factors of which require further investigation.

4.2 TIME-DEPENDENT TESTS

4.2.1 CREEP TEST

The ratio P/P_0 of the clamping force P(t) to the initial clamping force P_0 is shown in Fig.14 and 15. In the white oak specimen, WO-○12 and WO-□12 showed almost similar trends as there was no significant difference in the test conditions, but WO-○3 showed a lower P/P_0, which is considered to be influenced by the washer thickness.

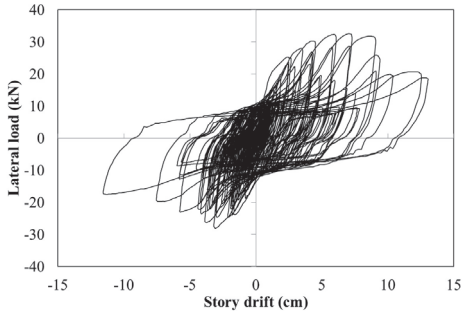

Figure 10. Load-displacement response.

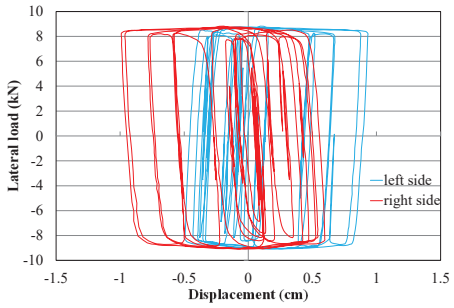

Figure 12. Connection displacement-lateral load relationships.

There were no significant differences in the Sugi specimens, although the P/P_0 trends were slightly different.

An analytical model has been proposed for the calculation of prestressing loss ΔP of prestressed wood from the balancing of wood and bolt deformations [4], and if ΔP is known, the creep coefficient $\phi_{\parallel}$ (t) of wood can be obtained by the following equation if the creep of the load cell is ignored.

$$\phi_{\parallel}(t) = \frac{-P_0\frac{l_p r_p}{E_p A_p\left(1-\chi_p r_{p(t)}\right)} - \Delta P(t)\left\{\frac{l_{\parallel}}{E_{\parallel}A_{\parallel}} + \frac{l_{lc}}{E_{lc}A_{lc}} + \frac{l_p}{E_p A_p\left(1-\chi_p r_p(t)\right)}\right\}}{\frac{\left(P_0+\Delta P(t)\chi_{\parallel}\right)l_{\parallel}}{E_{\parallel}A_{\parallel}}} \quad (1)$$

P_0: initial clamping force, ∥: parallel to the grain direction, *lc*: load cell, *p*: steel, *l*: length, *E*: Young's modulus, *A*: cross-sectional area, *r*: relaxation factor, χ: ageing coefficient

The creep coefficients obtained from (1) are shown in Fig 16 and 17, along with creep coefficients obtained from creep tests. Note that χ_p=0.8, $\chi_{\parallel}$=0.8 and r_p was obtained separately from the stress relaxation test of the bolt. The creep coefficients of WO-○12 and WO-□12 showed basically the same trend. On the other hand, since the apparent Young's modulus decreased to 41% when the washer thickness was as thin as 3 mm in a separate compression test, the WO-○3 was calculated with the Young's modulus reduced to 41%, resulting in creep modulus equivalent to WO-○12 and WO-□12. The creep coefficients obtained from the spring creep tests were

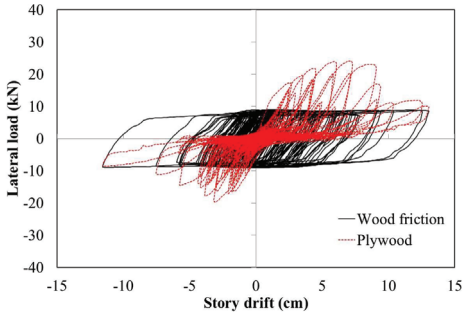

Figure 11. Load-displacement responses obtained from the strain gauges.

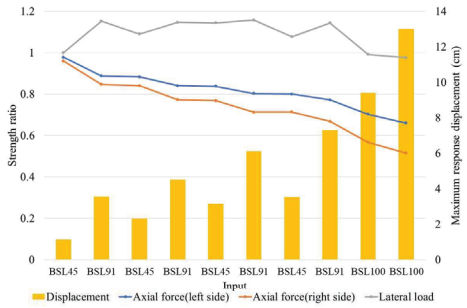

Figure 13. Strength ratio.

https://doi.org/10.52202/080513-0014

highly variable and therefore encompassed the creep coefficients determined by (1). In the Sugi specimen, a large difference occurred between SG-L and SG-M. Since there is no difference between the creep coefficients of SG-L-Cp and SG-M-Cp, the difference between SG-L and SG-M is probably due to the damage zones, which resulted in a higher creep coefficient for SG-M with a shorter specimen length.

4.2.2 CREEP TEST IN CYCLIC HUMIDITY

Wood creep is given as the sum of pure creep (φ_c) and mechanosorptive creep (φ_{ms}) by the following equation [4, 5]

$$\phi(t) = \phi_c(t) + \phi_{ms,r}(t,U) \quad (2)\ ,\ \phi_c = at^b \quad (3)$$

$$\phi_{ms,r}(t,U) = \phi^{\infty}\left[1 - e^{-cUt/(100\Delta t)}\right] + m_{ms}\Delta U_m \quad (4)$$

$$U = \int_0^{\Delta t} |du(\tau)| \quad (5)$$

ϕ^{∞}, c, m_{ms}: material parameters, U: accumulation of timber moisture variation over a period of time Δt, ΔU_m: moisture levels that were not attained during the previous load history

The ratio of the clamping force P to the clamping force P_c for each specimen with reference to the time at which the humidity variation started is shown in Fig. 18. The incremental creep coefficient calculated from prestress loss using (4) for one cycle of two weeks with humidity variation, and the variation in moisture content, is shown in Fig. 19. Note that the increase in the coefficient due to pure creep has been subtracted. Fig. 19 shows that the effect of humidity fluctuations is greater for Cy-SG25. The increase in creep was greatest during the first humidity change, and tended to gradually converge with subsequent humidity changes. This suggests that it is reasonable to divide mechanosorptive creep into recoverable with creep limit model (the first term on the right-hand side of (4)) and irrecoverable (the second term on the right-hand side of (4)). The parameters of (4) obtained from the results are shown in Table 5, and these values are used to determine P/P_0 by the analytical model. In the analytical model, the prestress loss as it varies with time is represented using the principle of superposition, but because of the integral term, it is represented in a closed form using the aging coefficient χ. Therefore, the ageing coefficient χ_p of the bolts was set to 0.8 [6] and the ageing coefficient χ of the wood was set to 0.9 (SG) and 0.95 (WO) by comparing the results of the calculations using the superposition principle (Fig. 20). P/P_c calculated from the analytical model is shown in Fig. 18. The experimental and analytical results were in close agreement.

3.2.3 PRESTRESS TEST IN UNCONTROLED ENVIRONMENT

The analytical results of the prestress loss in an uncontrolled environment are shown in Fig. 21 and 22, along with the experimental results. As V-2WO38 is tightened immediately after the wood dowel has dried and shrunk, however, the axial force increases due to the increase in moisture content after tightening, so the model (WO) was evaluated with m_{ms} = 0. Fig. 21 and 22 show that the experimental and analytical results are in good agreement.

6 – CONCLUSION

The dynamic and long-term performance of the friction-based connectors using longitudinal compression of wooden dowels were investigated. In the shake table test, the wall with friction-based connectors exhibited a bilinear hysteresis loop, reflecting the characteristics of the connectors. Although the clamping force of the connectors tended to decrease as the input progressed, the lateral load of the wall did not decrease, thus the factors

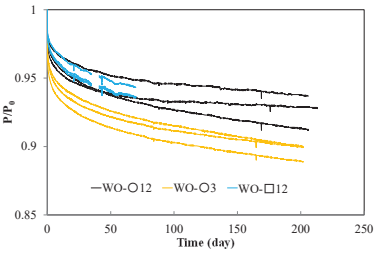

Figure 14.P/P_0 (White oak).

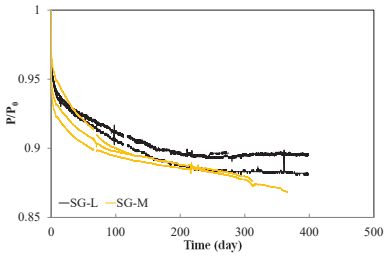

Figure 15.P/P_0 (Sugi).

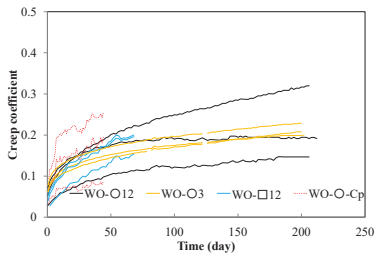

Figure 16.Creep coefficient (White oak).

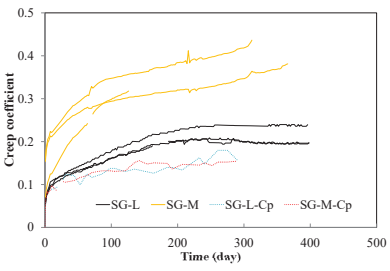

Figure 17. Creep coefficient (White oak).

https://doi.org/10.52202/080513-0014

that contributed to the decrease need further investigation. In the evaluation of the long-term performance of friction-based connectors, the loss of wood clamping force was evaluated using the analytical model. The longitudinal pure creep of wood required for the analysis was back-calculated using the analytical model from the prestress loss of wood in a constant temperature and humidity environment. The coefficients of mechanosorptive creep for moisture content variation were obtained from prestressed wood under the cyclic humidity environment by back-calculating the analytical model. The obtained creep coefficients were used to analyze the prestress loss of wood in an uncontrolled temperature and humidity environment, and the experimental and analytical results were in good agreement.

7 – REFERENCES

[1] Y. Wakashima, H. Shimizu, K. Ishikawa, Y. Fujisawa, S. Tesfamariam. “Friction-based connectors for timber shear walls: static experimental tests.” In: J Archit Eng 2019;25(2):04019006.

[2] Y. Wakashima, K. Ishikawa, H. Shimizu H, A. Kitamori, D. Matsubara, S. Tesfamariam. “Dynamic and long-term performance of wood friction connectors for timber shear walls.” In: Eng Struct 2021;241(12):112351.

[3] Y. Wakashima, K. Ishikawa, H. Shimizu, A. Kitamori, D. Matsubara, S. Tesfamariam. “Friction-based connectors with wooden dowels for timber shear walls: Shake table and time-dependent test” In:Eng. Struct., (2021), 241:112351.

[4] M. Fragiacomo, M. Davies. ”Long-Term Behavior of Prestressed LVL Members. II: Analytical Approach” In: J. Struct. Eng., (2011), 137 (12), 1562–1572 .

[5] T. Toratti. “Creep of timber beams in variable environment” (1992), Rep. No. 31. Helsinki, Finland: Helsinki Univ. of Technology.

[6] G. Granello, C. Leyder, A. Palermo, A. Frangi, S. Pampanin. “Design approach to predict post-tensioning losses in post-tensioned timber frames.” In: J. Struct. Eng., (2018), 144(8): 04018115

Tabe 5: Mechano-sorptive parameters

Parameter	Cy-SG25	Cy-WO40
ϕ_∞	0.4	0.15
c	6	5
m_{ms}	0.25	0.06

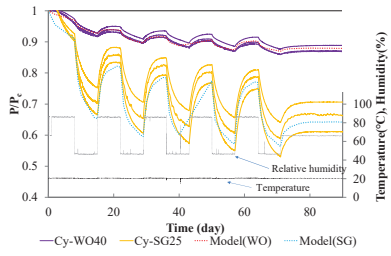

Figure 18. P/Pc in cyclic humidity.

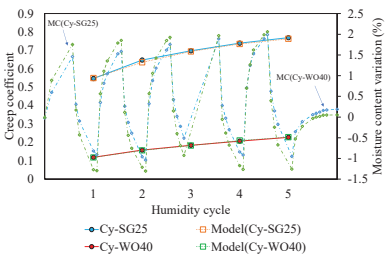

Figure 19. Mechanosorptive creep.

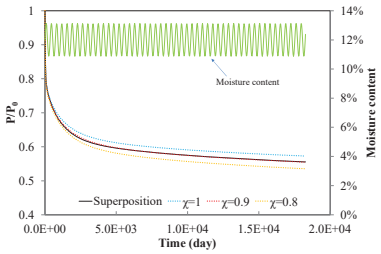

Figure 20. Ageing coefficient (SG).

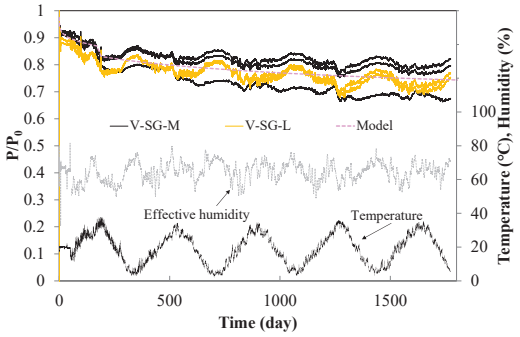

Figure 21. P/P0 in uncontrolled environment (SG).

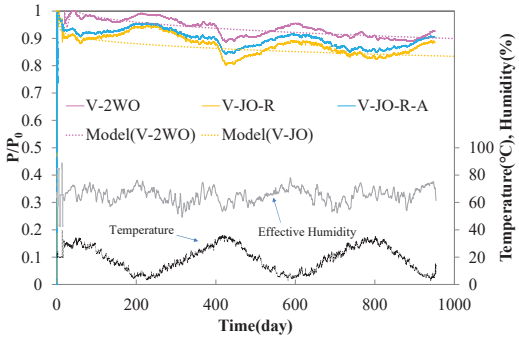

Figure 22. P/P0 in uncontrolled environment (WO, JO).

https://doi.org/10.52202/080513-0014